Observational Study

Medicine®

OPEN

Influence of the lamina cribrosa on the rate of global and localized retinal nerve fiber layer thinning in open-angle glaucoma

Hae-Young Lopilly Park, MD, PhD*, Sung In Kim, MD, Chan Kee Park, MD, PhD

Abstract

The advent of optical coherence tomography (OCT) imaging allows identification of the structural contribution of the lamina cribrosa (LC) to glaucoma progression. This study aimed to determine the role of various LC features, such as the LC depth (LCD), LC thickness (LCT), and focal LC defects, on the future rate of progressive retinal nerve fiber layer (RNFL) thinning in patients with glaucoma. One hundred eighteen patients with glaucoma who had undergone at least 4 OCT examinations were included. Features of LC, including the LCD, LCT, and presence of focal LC defects, from serial scan of the optic disc using the enhanced depth imaging of Spectralis OCT; were analyzed at baseline. Eyes were classified as those with or without progressive RNFL thinning using the guided progression analysis of Cirrus OCT. Factors associated with the rate of RNFL thinning (linear regression analysis against time for global average, inferior, and superior RNFL thicknesses, μm/year) were evaluated using a general linear model. Greater baseline LCD and thinner baseline LCT were significantly associated with the rate of superior RNFL thinning. Focal LC defects were significantly more frequent in eyes with progressive inferior RNFL thinning (93.8%) and the location of the focal LC defect was only related to the location of progression RNFL thinning in the inferior region ($P < 0.001$). A deeper and thinner LC was related to the rate of superior RNFL thinning, and the presence of focal LC defects was related to the rate of inferior RNFL thinning.

Abbreviations: LC = lamina cribrosa, LCD = lamina cribrosa depth, LCT = lamina cribrosa thickness, RNFL = retinal nerve fiber layer, OCT = optical coherence tomography, IOP = intraocular pressure.

Keywords: glaucoma, lamina cribrosa, retinal nerve fiber layer thinning

1. Introduction

Risk factors for the development and progression of glaucoma include elevated intraocular pressure (IOP), older age, advanced glaucoma stage, lower central corneal thickness, decreased ocular perfusion pressure, and the presence of disc hemorrhage (DH).[1,2] The structural features of the lamina cribrosa (LC) were recently investigated as potential risk factors for glaucoma progression. Focal LC defects were associated with glaucomatous visual field (VF) progression. Eyes with LC defects tended to progress faster than eyes without LC defects.[3] A thinner, deeper LC was significantly associated with the rate of progressive retinal nerve fiber layer (RNFL) thinning.[4] Posterior LC displacement was prominent in preperimetric and mild-to-moderate glaucoma when different glaucoma stages were compared.[5] However, the roles of the LC findings and how they may contribute to glaucoma progression remain to be determined.

With the advent of spectral-domain optical coherence tomography (OCT) with enhanced depth imaging (EDI), several studies have identified characteristics of the LC.[6–8] Park[8] proposed that structural characteristics of the LC in patients with glaucoma can occur in both generalized and localized patterns. The LC depth (LCD) and LC thickness (LCT), which could be one of generalized characteristics of the LC, are reported to be associated with age and IOP.[9–13] Focal LC defects, which could be one of focal characteristics of the LC, are reported to be associated with localized RNFL defects, DH, normal-tension glaucoma diagnosis, and myopic refractive errors.[14–17] Because the related factors differ between generalized and focal LC characteristics, we hypothesized that these characteristics may have different roles in glaucoma progression. The purpose of this study was to determine the role of generalized LC characteristics, as assessed by LCD and LCT, and focal LC characteristics, as assessed by the presence of focal LC defects, on the future rate of progressive RNFL thinning in patients with glaucoma.

2. Methods

2.1. Study subjects

This study was approved by the Institutional Review Board of Seoul St. Mary's Hospital, Seoul, South Korea and followed the

Editor: Marcella Nebbioso.

Funding/support: This work was supported by the National Research Foundation of Korea (NRF) grant, funded by the Korean government (MSIP; No.NRF-2014R1A1A3049403).

For the prospective component, ethical approval was obtained from the Institutional Review Board of Seoul St. Mary's Hospital, Seoul, South Korea. The study was conducted according to the principles set out in the Declaration of Helsinki. Written informed consent was obtained from all prospective patients before inclusion in the study, which was conducted according to the tenets of the Declaration of Helsinki.

The authors have declared that no conflict of interest exists.

Department of Ophthalmology, Seoul St. Mary's Hospital, College of Medicine, The Catholic University of Korea, Seoul, Korea.

* Correspondence: Chan Kee Park, Department of Ophthalmology, Seoul St. Mary's Hospital, College of Medicine, The Catholic University of Korea, Seoul, South Korea, 505 Banpo-dong, Seocho-ku, Seoul 137-701, Korea (e-mail: ckpark@catholic.ac.kr).

Medicine (2017) 96:14(e6295)

Received: 29 November 2016 / Received in final form: 4 February 2017 / Accepted: 13 February 2017

http://dx.doi.org/10.1097/MD.0000000000006295

tenets of the Declaration of Helsinki. Written informed consent was obtained from consecutive patients who met the eligibility criteria and were willing to participate in the study.

We prospectively enrolled patients with glaucoma from the glaucoma clinic of Seoul St. Mary's Hospital starting in March 2009. These patients were part of the CMC Suspect Cohort Study, an ongoing study that has been conducted since March 2009. Patients who had undergone at least 4 OCT examinations (Cirrus OCT; Carl Zeiss Meditec, Inc., Dublin, CA) with follow-up at for least 3 years were selected for this study. Each participant underwent a comprehensive ophthalmic assessment, including measurement of best-corrected visual acuity, refraction, slit-lamp biomicroscopy, gonioscopy, Goldmann applanation tonometry, central corneal thickness using ultrasound pachymetry (Tomey Corporation, Nagoya, Japan), determination of axial length using ocular biometry (IOL Master; Carl Zeiss Meditec, Inc., Dublin, CA), dilated stereoscopic examination of the optic disc and fundus, color disc photography, red-free RNFL photography (Canon, Tokyo, Japan), and Humphrey VF examination using the 24-2 Swedish Interactive Threshold Algorithm Standard program (Carl Zeiss Meditec, Inc., Dublin, CA). All patients were followed every 3 to 6 months with regular follow-up, including slit-lamp biomicroscopy, Goldmann applanation tonometry, and optic disc examination for DH detection. Color disc and fundus photography and Cirrus OCT examinations were usually repeated at intervals ranging from 6 to 12 months.

For a glaucoma diagnosis, patients had to fulfill the following criteria: glaucomatous optic disc appearances (such as diffuse or localized rim thinning, a notch in the rim, or a vertical cup-to-disc ratio higher than that of the other eye by >0.2) and glaucomatous VF loss (defined as the consistent presence of a cluster of ≥3 nonedge points on the pattern deviation plot with a probability of occurring in <5% of the normal population, with one of these points having the probability of occurring in <1% of the normal population, a pattern standard deviation with $P<5\%$, or a Glaucoma Hemifield Test result outside the normal limits in a consistent pattern on 2 qualifying VFs), confirmed by 2 glaucoma specialists (HYP and CKP), in addition to an open angle on gonioscopic examination.

To be included in the study, patients were required to meet the following inclusion criteria: a best-corrected visual acuity of ≥20/40, a spherical refraction within ±6.0 diopters, a cylinder correction within ±3.0 diopters, consistently reliable VFs (defined as false-negative rate of <15%, false-positive rate of <15%, and fixation losses of <20%), and a mean deviation worse than –30.00 dB. Patients were excluded on the basis of any of the following criteria: a history of any retinal diseases; a history of eye trauma or surgery, with the exception of uncomplicated cataract surgery; a glaucoma incisional surgery or laser procedure; another optic nerve disease besides glaucoma; or a history of systemic or neurological diseases that might affect the VF. One eye was randomly selected from each patient with glaucoma who met the inclusion and exclusion criteria if both eyes were eligible.

We recorded the age at the time of EDI OCT and baseline VF mean deviation at the initial visit. The IOPs were recorded at each visit. Baseline untreated IOP was the initial-visit IOP with no glaucoma medication. The mean IOP during the entire follow-up period was calculated by averaging all measurements. The IOP fluctuation was defined as the standard deviation of this value. DH was defined as an isolated flame-shape or splinter-like hemorrhage on the optic disc or peripapillary area, extending to the border of the optic disc. Stereoscopic disc photographs and medical records were reviewed for the presence of DH.

2.2. Enhanced-depth imaging optical coherence tomography

At the time of enrollment, serial horizontal and vertical cross-sectional scans covering the optic nerve head (ONH), approximately 30 μm apart, were obtained using the EDI technique of the Spectralis OCT (Heidelberg Engineering, GmbH, Dossenheim, Germany) for LC analyses, as described previously.[6,7,18] Images with a quality score >15 were obtained (approximately 65–70 sections per eye).

First, the EDI OCT images were reviewed for the presence of focal LC defects that violated the smooth curvilinear U- or W-shaped cross-sectional contour of the LC.[14,15,17,19,20] Experienced glaucoma specialists (HYP and SIK), blinded to the patients' clinical information and infrared optic disc photographs, performed this review. Focal characteristics of the LC were defined using the guidelines specified by Kiumehr et al[15] Focal LC defects were considered to be present when violating the curvilinear U- or W-shaped contour of the anterior LC surface was observed. The diameter of the defects at their opening was required to be ≥100 μm in diameter and >30 μm in depth.[15] In addition, to be considered as focal LC defects, the LC findings had to be present in 2 neighboring B-scans to avoid false positives in both the horizontal and vertical scans (Fig. 1, indicated in green lines). The location of the focal LC defect was classified into superior or inferior region according to the location of the B-scan in which the defect was found. To assess the intraobserver reproducibility of focal LC defect evaluation, EDI OCT images of 50 randomly selected glaucomatous eyes were evaluated. Analysis was based on 3 independent series of re-evaluations. The absolute agreement of the single observer's evaluation was calculated with the intraclass correlation coefficient from a 2-way mixed effects model.

Next, the LCD and LCT were measured at 3 locations (midhorizontal, superior, and inferior midperipheral regions of the ONH). The LCD was determined by measuring the distance from the opening plane of Bruch membrane (BM) to the level of the anterior LC surface. The reference line connecting the 2 termination points of the BM edges was used as a reference plane and was drawn in each B-scan image (Fig. 1, red glyphs and red line). The distance from the reference line to the level of the anterior border of the LC was measured at 3 points (the maximally depressed point and 2 additional points, 100 and 200 μm temporally from the maximally depressed point). The average of the 9 measurements, 3 values from each 3 location, was used as the LCD (Fig. 1, 3 red perpendicular lines). The LCT was measured as the distance between the anterior and posterior borders of the LC in the direction perpendicular to the anterior LC surface at the measurement point (Fig. 1, yellow line between yellow glyphs marking the anterior and posterior borders of the LC). The average of 3 values from 3 locations was used as the LCT. The measurement of the LCD and LCT were classified into superior and inferior LCD/LCT according to the measured location. Average of 3 measurements for LCD and 1 measurement of LCT was considered as superior and inferior LCD/LCT. To assess intraobserver reproducibility of the measurement of LCD and LCT, EDI OCT images of 100 randomly selected glaucomatous eyes were evaluated. Analysis was based on 3 independent series of re-evaluations. The absolute agreement of the single observer's evaluation was calculated with the intraclass correlation coefficient from 2-way mixed effects model.

2.3. Cirrrus optical coherence tomography

RNFL thickness was measured using the optic disc cube protocol of a Cirrus OCT running version 6.0 software (Cirrus OCT; Carl

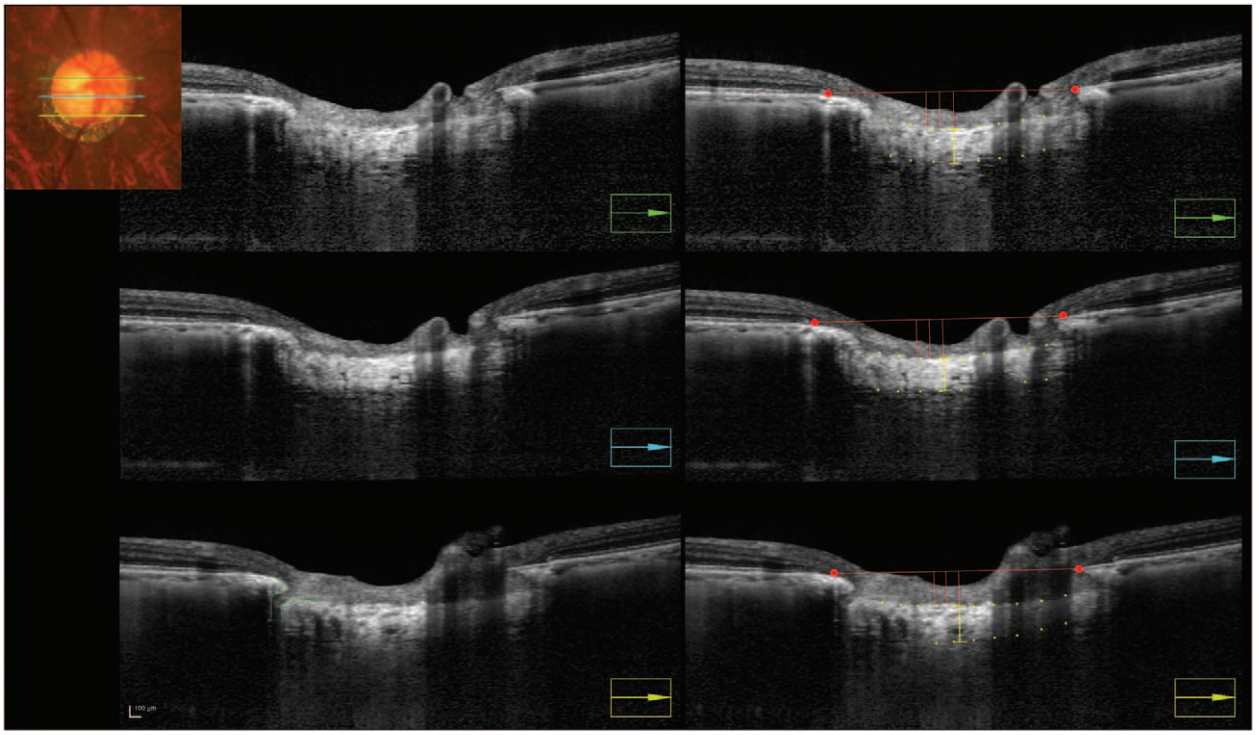

Figure 1. Enhanced depth imaging of the optic nerve head using Spectralis optical coherence tomography was performed at the time of enrollment. A focal lamina cribrosa (LC) defect was considered as a violation of the curvilinear U- or W-shaped contour of the anterior LC surface (green outline). It had to be identified in 2 neighboring B-scans with their opening to be ≥100 μm in diameter and >30 μm in depth. Both LC depth (LCD) and LC thickness (LCT) were measured at three locations (superior midperipheral, green arrow; midhorizontal, blue arrow; inferior midperipheral, yellow arrow). The LCD was determined by measuring the distance from the Bruch membrane (BM) opening plane to the level of the anterior LC surface. The reference line (red line) connecting the 2 termination points of the BM edges (red glyphs) was used as a reference plane and was drawn in each B-scan image. The distance from the reference line to the level of the anterior border of the LC was measured at 3 points in each location (the maximally depressed point and 2 additional points, 100 and 200 μm temporally from the maximally depressed point). The average of the 3 values was used as the LCD (three red perpendicular lines) at that location. The LCT was measured as the distance between the anterior and posterior borders of LC in the direction perpendicular to the anterior LC surface at the measurement point (yellow line between yellow glyphs marking the anterior and posterior border of the LC). The average of 3 values from 3 locations was used as the mean LCD and mean LCT.

Zeiss Meditec, Inc., Dublin, CA). The Optic Disc Cube protocol scans a $6 \times 6\,mm^2$ area centered on the ONH and collects 200×200 axial scans containing 40,000 points. Images exhibiting involuntary saccade, misalignment, or blinking artifacts and those with a signal strength of <6 were discarded. Images featuring algorithm segmentation failure were also excluded after visual inspection.

Eyes were classified as those with or without progressive RNFL thinning using the guided progression analysis (GPA) software of Cirrus OCT. At least 4 OCT examinations are necessary to generate a GPA report, which was an inclusion criterion for this study. The superior and inferior RNFL thicknesses are plotted against the duration of follow-up. If progression was suspected, the RNFL thickness at each visit was indicated as "possible loss" or "likely loss." Progression was identified if the observed change from baseline (the first 2 OCT examinations) to a test value exceeds the test–retest variability of the system. If the "'possible loss" criterion was met on 2 successive visits, that patient was considered to show "likely loss." We considered that "likely loss" in either the superior or inferior region reflected progressive RNFL thinning and thus glaucomatous progression.

2.4. Statistical analysis

All data are presented as mean ± standard deviation. Linear regression analysis against time was performed for the global average, inferior, and superior RNFL thicknesses for each patient to determine the rate of change in the RNFL thickness (expressed in μm/year). A general linear model was used to identify factors associated with the rate of change in RNFL thickness. The dependent variable was the rate of RNFL thinning in the global, inferior, and superior regions. The independent variables exhibiting significance at $P < 0.10$ in the univariate model were included in the multivariate model. A P value of < 0.05 was considered to indicate statistical significance. Statistical analyses were performed using the SPSS software (ver. 16.0; SPSS Inc., Chicago, IL).

3. Results

In total, 127 eyes of 127 patients with open-angle glaucoma who met the inclusion and exclusion criteria were included. Of these 127 eyes, 9 (7.1%) were excluded from further analysis because of poor OCT scan images of the LC or unable to measure the LC thickness. The remaining 118 eyes were analyzed. All 118 eyes were under treatment to lower the IOP (72.8% on prostaglandins). The mean number of evaluated OCTs was 5.87 ± 0.70, with a mean follow-up of 4.18 ± 0.79 years. Focal LC defects were present in 66 of 118 (55.9%) eyes. Among these focal LC defects, 29 (24.6%) eyes were located in the superior region and 37 (31.4%) in the inferior region. The mean LCD and LCT were 425.35 ± 138.50 (range, 146–914) μm and 242.05 ± 46.14 (range, 150–410) μm, respectively. Detection of the presence

Table 1

Patient clinical characteristics.

Age, y	53.27 ± 13.23 (31–75)
Sex, Female:Male	52:66
Spherical equivalent, diopters	−3.24 ± 3.10 (−6 to 1.5)
Axial length, mm	24.85 ± 1.67 (22.4–27.2)
Untreated baseline IOP, mm Hg	16.65 ± 3.88 (11–32)
Mean follow-up IOP, mm Hg	14.39 ± 3.14 (9–21)
IOP fluctuation, mm Hg	1.57 ± 1.02 (0–5)
Central corneal thickness, μm	542.81 ± 31.25 (483–619)
Baseline visual field MD, dB	−4.76 ± 0.48 (−29.6 to 0.8)
Baseline visual field PSD, dB	4.65 ± 3.12 (1.2–13.4)
Baseline global RNFL thickness	78.26 ± 13.45 (51–108)
Number of eyes with disc hemorrhage, n (%)	31 (26.3%)
Mean LCD, μm	425.35 ± 138.50 (146–914)
Mean LCT, μm	242.05 ± 46.14 (150–410)
Number of eyes with focal LC defect, n (%)	66 (55.9%)
Superior focal LC defect, n (%)	29 (24.5%)
Inferior focal LC defect, n (%)	37 (31.4%)
Rate of global RNFL thinning, μm/y	−0.88 ± 2.48 (−6.0 to 3.5)
Rate of superior RNFL thinning, μm/y	−1.73 ± 4.09 (−11.0 to 2.2)
Rate of inferior RNFL thinning, μm/y	−2.14 ± 3.04 (−16.5 to 2.0)
Mean follow-up duration, y	4.18 ± 0.79 (3–6)
Average OCT scans per eye, n	5.87 ± 0.70 (4–6)

Data are mean ± standard deviation (range) unless otherwise indicated.

IOP = intraocular pressure, LC = lamina cribrosa, LCD = lamina cribrosa depth, LCT = lamina cribrosa thickness, MD = mean deviation, OCT = optical coherence tomography, PSD = pattern standard deviation, RNFL = retinal nerve fiber layer.

of focal LC defects and measurements of LCD and LCT showed excellent intraobserver reproducibility. The intraclass correlation coefficient for focal LC defect evaluation was 0.973 [95% confidence interval (95% CI) = 0.962–0.985], 0.960 (95% CI = 0.951–0.973) for LCD measurements and 0.939 (95% CI = 0.919–0.952) for LCT measurements. The patients' clinical characteristics are summarized in Table 1.

The global rate of RNFL thinning in all eyes was –0.88 ± 2.48 (range, –6.0 to 3.5) μm/year. The rate of RNFL thinning was –1.73 ± 4.09 (range, –11.0 to 2.2) μm/year in the superior region and –2.14 ± 3.04 (range, –16.5 to 2.0) μm/year in the inferior region. Factors associated with the rate of superior and inferior RNFL thinning were evaluated using a general linear model. When factors associated with the rate of superior RNFL thinning were evaluated, a greater baseline LCD and thinner baseline LCT were the only factors significantly associated in both univariate and multivariate analyses (Table 2). When factors associated with the rate of inferior RNFL thinning were evaluated, a greater baseline pattern standard deviation of the VF, DH during follow-up, and the presence of focal LC defects showed statistically significant relationships in the univariate analysis. The presence of DH during follow-up and the presence of focal LC defects at baseline were significantly associated with inferior RNFL thinning in the multivariate analysis (Table 3).

A scatterplot indicating the relationship between the rate of RNFL thinning and the LC parameters (mean LCD and LCT) is shown in Fig. 2. The rate of global RNFL thinning showed a significant linear relationship with the LCD ($R^2 = 0.037$, $P = 0.038$) and LCT ($R^2 = 0.085$, $P = 0.001$). However, the relationship between the LCD and rate of superior RNFL thinning was stronger ($R^2 = 0.273$, $P < 0.001$). There was no significant relationship between the LC parameters and the rate of inferior RNFL thinning. There was no significant relationship between the LC parameters and the rate of inferior RNFL thinning. Subgroup analyses between eyes with and without focal LC defects are shown in Fig. 3. The relationship with the rate of inferior RNFL thinning in eyes without focal LC defects showed that a deeper LCD and thinner LCT were related to more rapid RNFL thinning, although the relationship was statistically significant only with the LCT. However, in eyes with focal LC defects, the rate of inferior RNFL thinning showed no relationship with the LCD or LCT.

Eyes were classified into progressive or nonprogressive RNFL thinning groups using the GPA analysis of the Cirrus OCT. Eyes with progressive superior RNFL thinning showed significant differences in the superior LCD and superior LCT ($P = 0.005$ and $P = 0.001$) compared with eyes without superior RNFL progression. The frequency of focal LC defects or the superiorly located focal LC defects did not differ between eyes with or without progressive superior RNFL thinning ($P = 0.216$ and $P = 0.537$). However, eyes with progressive inferior RNFL thinning, focal LC

Table 2

Factors associated with the rate of superior retinal nerve fiber layer thinning.

	Univariate analysis			Multivariate analysis		
	β	95% CI	*P*	β	95% CI	*P*
Age per 1 y older	−0.069	−0.163 to 0.024	0.144			
Axial length per 1 mm longer	0.359	−0.327 to 1.045	0.298			
Central corneal thickness per 1 μm thicker	−0.011	−0.048 to 0.027	0.580			
Baseline untreated IOP per 1 mm Hg higher	−0.015	−0.284 to 0.254	0.910			
Mean IOP during follow-up period per 1 mm Hg higher	−0.002	−0.227 to 0.223	0.985			
IOP fluctuation during follow-up period per 1 mm Hg higher	−0.038	−0.753 to 0.677	0.917			
Visual field MD per 1 dB higher	−0.082	−0.301 to 0.137	0.457			
Visual field PSD per 1 dB higher	0.238	−0.015 to 0.462	0.137			
Disc hemorrhage	−1.267	−2.897 to 0.364	0.127			
Average RNFL thickness per 1 μm thicker	−0.049	−0.138 to 0.040	0.277			
Mean LCD per 1 μm larger	−0.525	−0.111 to −0.907	**<0.001**	−0.512	−0.121–0.903	**<0.001**
Mean LCT per 1 μm thicker	0.170	0.001 to 0.320	**0.068**	0.228	0.002–0.353	**0.033**
Presence of focal LC defect	1.068	−1.327 to 3.463	0.376			
Follow-up period per 1 y longer	0.000	−0.882 to 0.883	0.999			
Number of OCT RNFL scans per 1 more scan	−0.215	−1.243 to 0.813	0.679			

Factors with statistical significance are shown in boldface.

IOP = intraocular pressure, MD = mean deviation, LC = lamina cribrosa, LCD = lamina cribrosa depth, LCT = lamina cribrosa thickness, OCT = optical coherence tomography, PSD = pattern standard deviation, RNFL = retinal nerve fiber layer.

Table 3

Factors associated with the rate of inferior retinal nerve fiber layer thinning.

	Univariate analysis			Multivariate analysis		
	β	95% CI	*P*	β	95% CI	*P*
Age per 1 y older	−0.010	−0.095 to 0.116	0.848			
Axial length per 1 mm longer	0.482	−0.278 to 1.241	0.209			
Central corneal thickness per 1 μm thicker	−0.004	−0.046–0.038	0.844			
Baseline untreated IOP per 1 mm Hg higher	−0.008	−0.306 to 0.290	0.958			
Mean IOP during follow-up period per 1 mm Hg higher	−0.037	−0.211 to 0.137	0.675			
IOP fluctuation during follow-up period per 1 mm Hg higher	0.494	−0.052 to 1.040	0.076	0.453	−0.311 to 1.217	0.240
Visual field MD per 1 dB higher	0.188	−0.050 to 0.426	0.118			
Visual field PSD per 1 dB higher	−0.178	−0.351 to −0.005	**0.043**	−0.150	−0.377 to 0.078	0.192
Disc hemorrhage	−1.286	−2.538 to −0.033	**0.044**	−2.036	−3.711 to −0.361	**0.018**
Average RNFL thickness per 1 μm thicker	0.010	−0.089 to 0.109	0.869			
Mean LCD per 1 μm larger	−0.004	−0.012 to 0.005	0.423			
Mean LCT per 1 μm thicker	0.008	−0.025 to 0.025	0.661			
Presence of focal LC defect	−1.764	−3.311 to −0.217	**0.026**	−1.262	−2.761 to −0.237	**0.047**
Follow-up period per 1 y longer	−0.131	−0.814 to 0.552	0.704			
Number of OCT RNFL scans per 1 more scan	−0.233	−1.027 to 0.562	0.563			

Factors with statistical significance are shown in boldface.

IOP = intraocular pressure, LC = lamina cribrosa, LCD = lamina cribrosa depth, LCT = lamina cribrosa thickness, MD = mean deviation, OCT = optical coherence tomography, PSD = pattern standard deviation, RNFL = retinal nerve fiber layer.

defects were significantly more frequent in eyes with progressive inferior RNFL thinning (93.8%) than in eyes without progressive inferior RNFL thinning (50.0%, $P=0.001$).

4. Discussion

Our study demonstrated an association between LC features and the rate of RNFL thinning in patients with glaucoma. Importantly, deepening and thinning of the LC were risk factors for faster progression of global RNFL thinning, as reported previously.[4] However, this relationship differed when the region of RNFL thinning was considered. A deeper and thinner LC was significantly correlated to the rate of superior RNFL thinning. For the inferior region, the presence of a focal LC defect was the only LC feature that was correlated to the rate of RNFL thinning. The frequency of focal LC defects was significantly different between eyes with and without progressive inferior RNFL thinning, but was not different between eyes with and without progressive superior RNFL thinning. These findings showed that LC features contribute differently to glaucoma progression throughout the ONH region. Generally, a deeper and thinner LC is a risk factor for RNFL thinning. However, when focal LC features are present, especially in the inferior region of the LC, RNFL thinning mostly occurs in that susceptible region, whereas general features of the LC, such as deeper and thinner LC, contribute less to the rate of RNFL thinning in eyes with focal LC defects. In eyes

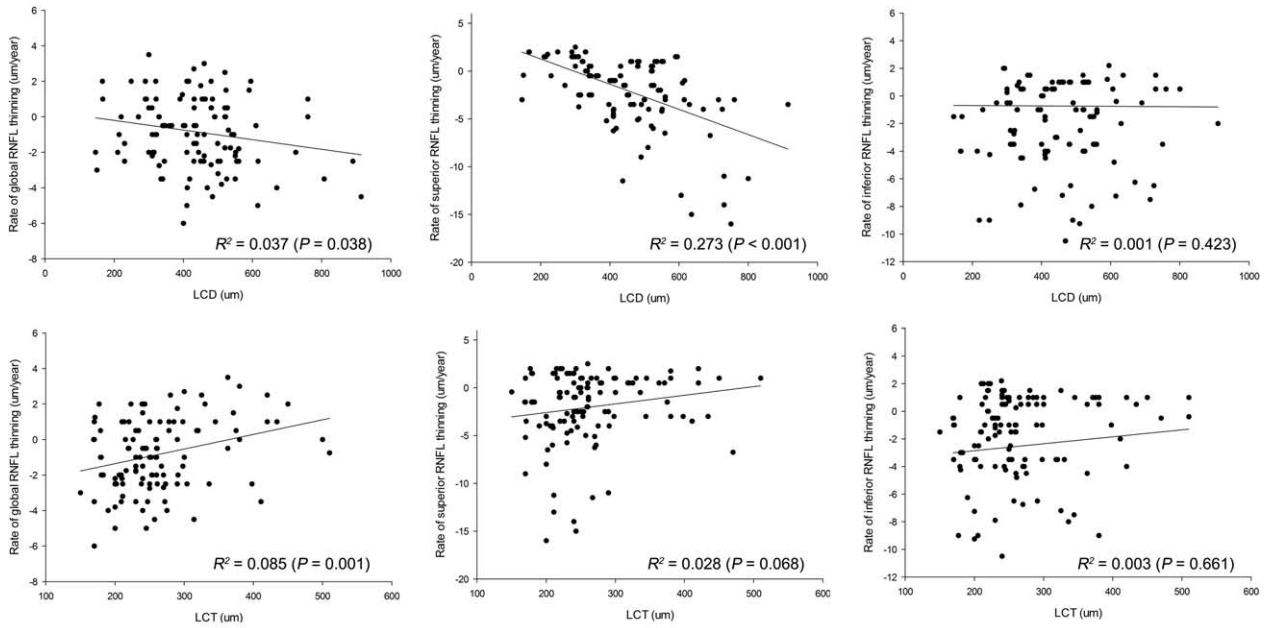

Figure 2. Scatterplot showing the relationship between the rate of retinal nerve fiber layer (RNFL) thinning and the lamina cribrosa depth (LCD) and the lamina cribrosa thickness (LCT). The relationships with global RNFL thinning (left), superior RNFL thinning (middle), and inferior RNFL thinning (right) are shown.

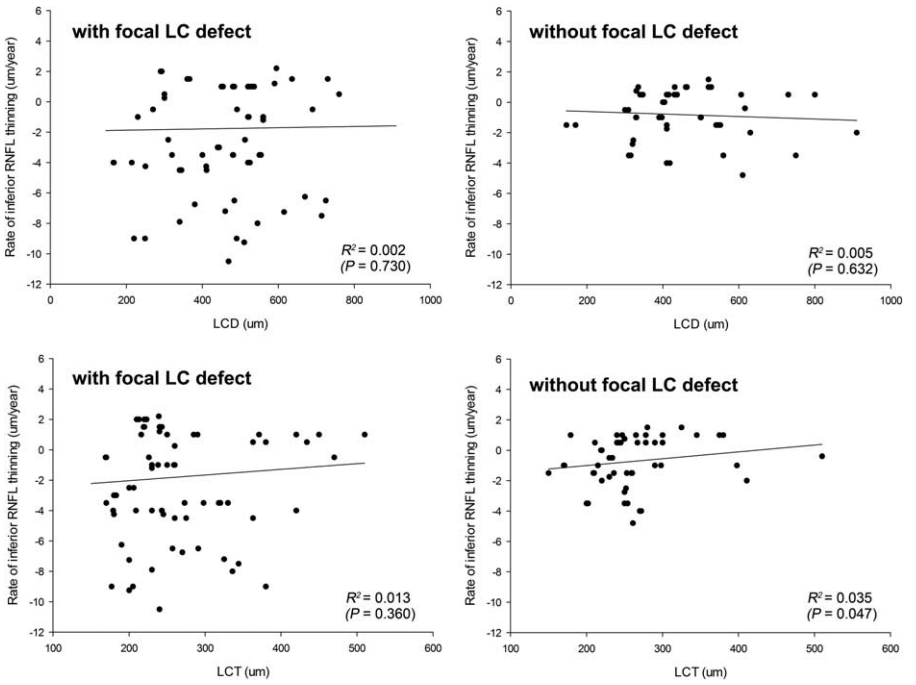

Figure 3. Scatterplot showing the relationship between the rate of inferior retinal nerve fiber layer thinning and the lamina cribrosa (LC) depth or the LC thickness in eyes with and without focal LC defects.

without focal LC defects, a deeper LCD and thinner LCT had relationships with the rate of inferior RNFL thinning similar to those of global and superior RNFL thinning. In eyes with focal LC defects, other parameters such as the LC defect size or depth may contribute to the rate of RNFL thinning; however, this was difficult to analyze because no standardized method with which to quantify LC defects has yet been established.

Previously, 100 μm deepening of mean LCD increased 35% of global RNFL thinning rate. Also, 100 μm thickening of mean LCT decreased 85% of global RNFL thinning rate.[4] Our data showed that 1 μm deepening of mean LCD was associated with 0.7% increase and 1 μm thickening of mean LCT was associated with 0.6% decrease in the rate of superior RNFL thinning. The findings of our study seem to have clinical significance. A previous study showed that eyes with VF progression showed a more frequent presence of focal LC defects.[16] This study showed that eyes with focal LC defects showed faster rates of both global and localized VF progression. The inferotemporal and superotemporal regions of the LC have larger pores with less connective tissue, increasing the likelihood of glaucomatous damage.[21,22] Because glaucomatous damage occurs more often in the inferotemporal and superotemporal regions, focal LC features observed in OCT images have been frequently identified in these regions.[15–17,23–25] Factors related to the rate of inferior RNFL thinning were the presence of DH and focal LC defects, which were also related to each other in other studies.[14–17] Because focal LC defects are associated with more rapid localized VF progression and progressive inferior RNFL thinning, focal LC defects may indicate regional susceptibility of the LC. When a focal LC defect is present at baseline, localized changes in the VF and RNFL should be monitored more carefully. The reason why only the inferior region was associated with the presence of focal LC defects and not the superior region remains unclear. Some reports have suggested that the inferotemporal LC has less connective tissue and the larger pores than does the superotemporal LC and this contributes to the increased glaucoma susceptibility in the inferior region, followed by the superior disc region.[26–28] Hood et al[29] proposed that the inferior foveal location, relative to the optic disc, results in a distinct asymmetric distribution of the circumpapillary retinal nerve fiber layer between the superior and inferior retina. Particularly, "crowding" of the papillomacular bundles at the inferotemporal disc at the level of the LC occurs and increases susceptibility to glaucomatous damage.[29] Focal LC defects in the inferotemporal region could add susceptibility in that region where retinal ganglion cell axons are susceptible due to a "crowding effect."

However, generalized characteristics of the LC affect the rate of RNFL thinning globally and in the superior region. The LC demonstrates posterior bowing and compression during glaucomatous cupping.[30,31] By in vivo imaging of the LC using OCT, backward bowing could be observed as deepening of the LCD and compression as thinning of the LCT. The LCD and LCT, which could be generalized LC features, are reportedly associated with age and IOP.[9–13] The LCD correlated with baseline untreated IOP and LCD reduction was related to the degree of IOP reduction in several studies.[6,9,32] This could be summarized as follows: generalized LC features are mainly influenced by risk factors, such as IOP and age, which have been reported to be major risk factors for global glaucoma progression. When eyes have no focal LC features by LC imaging, the LCD and LCT can be used as significant risk factors to predict progressive RNFL thinning in the global and superior region. The reason for the significant association of the LCD and LCT parameter for only the superior region in terms of RNLF thinning, not in the inferior region, may be a result of the anatomy of the LC. The anterior LC insertion is reported to be deeper in the superior than inferior region in both glaucoma and normal control eyes.[33] This LC insertion was shown to be located more posteriorly in glaucomatous eyes, suggesting posterior migration of the LC insertion, and it was more

prominent in the superior than inferior region. Computer modeling studies have shown that more deeply located LC is exposed to increased strain within the tissue and is thought to be more susceptible to glaucomatous changes.[34,35] This could be one reason for the contribution of the LCD and LCT only to superior RNLF thinning.

Our findings may describe the clinical features according to glaucoma types. Open-angle glaucoma with high IOP is reported to exhibit diffuse damage in the RNFL and VF compared with glaucoma with normal IOP.[36–42] These findings suggest that the backward bowing and posterior location of the LC by high IOP may be related to the pathogenic mechanism of diffuse glaucomatous damage in glaucoma with high IOP. In contrast, focal LC defects are localized changes of the LC. Focal laminar defects are more frequently found in glaucoma with normal IOP.[14–17,23,24] Glaucoma with normal IOP displays more localized and deeper damage in the superior VF region than does glaucoma with high IOP.[36–42] The progression pattern of glaucoma with normal IOP is reported to be faster in the superior VF region, consistent with our findings that eyes with focal LC defects showed faster inferior RNFL thinning.[43]

Our study has several limitations. First, only patients from a single ethnic group with glaucoma who were treated medically were included. Thus, these results may not be generalizable to all patients with glaucoma. Second, the follow-up period was relatively short. Further investigation is needed to determine the long-term influence of LC features on glaucoma progression. Third, issues of the poor visualization of the LC under the optic disc rim and vessels exist. It is possible that some LC alterations in areas with poor OCT penetration may have been missed. To reduce false-positive detection of focal LC defects, we defined a LC defect as having a diameter of $\geq$100 μm and a depth of $>$30 μm. The LC defect also had to be present in 2 neighboring B-scans. The definition of LC defects was based on previous studies and may not be ideal. However, previous studies have mentioned that the definition we used may exclude normal anatomical variations and artifacts.

In conclusion, our study shows that different LC features had different effects on regional RNFL thinning. Generalized characteristics of the LC, such as deeper and thinner LC at baseline, were related to future superior RNFL thinning. Focal characteristics of the LC, such as focal LC defects, were related to inferior RNFL thinning.

References

[1] Gordon MO, Beiser JA, Brandt JD, et al. The Ocular Hypertension Treatment Study: baseline factors that predict the onset of primary open-angle glaucoma. Arch Ophthalmol 2002;120:714–20. discussion 829–30.

[2] Leske MC, Heijl A, Hyman L, et al. Predictors of long-term progression in the early manifest glaucoma trial. Ophthalmology 2007;114:1965–72.

[3] Faridi OS, Park SC, Kabadi R, et al. Effect of focal lamina cribrosa defect on glaucomatous visual field progression. Ophthalmology 2014;121:1524–30.

[4] Lee EJ, Kim TW, Kim M, et al. Influence of lamina cribrosa thickness and depth on the rate of progressive retinal nerve fiber layer thinning. Ophthalmology 2015;122:721–9.

[5] Park SC, Brumm J, Furlanetto RL, et al. Lamina cribrosa depth in different stages of glaucoma. Invest Ophthalmol Vis Sci 2015;56:2059–64.

[6] Park HY, Shin HY, Jung KI, et al. Changes in the lamina and prelamina after intraocular pressure reduction in patients with primary open-angle glaucoma and acute primary angle-closure. Invest Ophthalmol Vis Sci 2014;55:233–9.

[7] Park HY, Jeon SH, Park CK. Enhanced depth imaging detects lamina cribrosa thickness differences in normal tension glaucoma and primary open-angle glaucoma. Ophthalmology 2012;119:10–20.

[8] Park SC. In vivo evaluation of lamina cribrosa deformation in glaucoma. J Glaucoma 2013;22(Suppl 5):S29–31.

[9] Jung KI, Jung Y, Park KT, et al. Factors affecting plastic lamina cribrosa displacement in glaucoma patients. Invest Ophthalmol Vis Sci 2014;55:7709–15.

[10] Lee EJ, Kim TW, Weinreb RN, et al. Reversal of lamina cribrosa displacement after intraocular pressure reduction in open-angle glaucoma. Ophthalmology 2013;120:553–9.

[11] Reis AS, O'Leary N, Stanfield MJ, et al. Laminar displacement and prelaminar tissue thickness change after glaucoma surgery imaged with optical coherence tomography. Invest Ophthalmol Vis Sci 2012;53:5819–26.

[12] Zhao Q, Qian X, Li L, et al. Effect of elevated intraocular pressure on the thickness changes of cat laminar and prelaminar tissue using optical coherence tomography. Biomed Mater Eng 2014;24:2349–60.

[13] Lee EJ, Kim TW, Weinreb RN, et al. Lamina cribrosa thickness is not correlated with central corneal thickness or axial length in healthy eyes: central corneal thickness, axial length, and lamina cribrosa thickness. Graefes Arch Clin Exp Ophthalmol 2013;251:847–54.

[14] Park SC, Hsu AT, Su D, et al. Factors associated with focal lamina cribrosa defects in glaucoma. Invest Ophthalmol Vis Sci 2013;54:8401–7.

[15] Kiumehr S, Park SC, Syril D, et al. In vivo evaluation of focal lamina cribrosa defects in glaucoma. Arch Ophthalmol 2012;130:552–9.

[16] You JY, Park SC, Su D, et al. Focal lamina cribrosa defects associated with glaucomatous rim thinning and acquired pits. JAMA Ophthalmol 2013;131:314–20.

[17] Tatham AJ, Miki A, Weinreb RN, et al. Defects of the lamina cribrosa in eyes with localized retinal nerve fiber layer loss. Ophthalmology 2014;121:110–8.

[18] Park HY, Park CK. Diagnostic capability of lamina cribrosa thickness by enhanced depth imaging and factors affecting thickness in patients with glaucoma. Ophthalmology 2013;120:745–52.

[19] Choi YJ, Lee EJ, Kim BH, et al. Microstructure of the Optic Disc Pit in Open-Angle Glaucoma. Ophthalmology 2014.

[20] Lee EJ, Kim TW, Kim M, et al. Recent structural alteration of the peripheral lamina cribrosa near the location of disc hemorrhage in glaucoma. Invest Ophthalmol Vis Sci 2014;55:2805–15.

[21] Dandona L, Quigley HA, Brown AE, et al. Quantitative regional structure of the normal human lamina cribrosa. A racial comparison. Arch Ophthalmol 1990;108:393–8.

[22] Quigley HA, Addicks EM, Green WR. Optic nerve damage in human glaucoma. III. Quantitative correlation of nerve fiber loss and visual field defect in glaucoma, ischemic neuropathy, papilledema, and toxic neuropathy. Arch Ophthalmol 1982;100:135–46.

[23] Choi YJ, Lee EJ, Kim BH, et al. Microstructure of the optic disc pit in open-angle glaucoma. Ophthalmology 2014;121:2098–106.e2.

[24] Kimura Y, Akagi T, Hangai M, et al. Lamina cribrosa defects and optic disc morphology in primary open angle glaucoma with high myopia. PLoS One 2014;9:e115313.

[25] Takayama K, Hangai M, Kimura Y, et al. Three-dimensional imaging of lamina cribrosa defects in glaucoma using swept-source optical coherence tomography. Invest Ophthalmol Vis Sci 2013;54:4798–807.

[26] Quigley HA, Addicks EM, Green WR, Maumenee AE. Optic nerve damage in human glaucoma. II. The site of injury and susceptibility to damage. Arch Ophthalmol 1981;99:635–49.

[27] Jonas JB, Fernandez MC, Sturmer J. Pattern of glaucomatous neuroretinal rim loss. Ophthalmology 1993;100:63–8.

[28] Jonas JB, Mardin CY, Schlotzer-Schrehardt U, Naumann GO. Morphometry of the human lamina cribrosa surface. Invest Ophthalmol Vis Sci 1991;32:401–5.

[29] Hood DC, Raza AS, de Moraes CG, et al. Glaucomatous damage of the macula. Prog Retin Eye Res 2013;32:1–21.

[30] Emery JM, Landis D, Paton D, et al. The lamina cribrosa in normal and glaucomatous human eyes. Trans Am Acad Ophthalmol Otolaryngol 1974;78:O290–7.

[31] Quigley HA, Hohman RM, Addicks EM, et al. Morphologic changes in the lamina cribrosa correlated with neural loss in open-angle glaucoma. Am J Ophthalmol 1983;95:673–91.

[32] Yoshikawa M, Akagi T, Hangai M, et al. Alterations in the neural and connective tissue components of glaucomatous cupping after glaucoma surgery using swept-source optical coherence tomography. Invest Ophthalmol Vis Sci 2014;55:477–84.

[33] Lee KM, Kim TW, Weinreb RN, et al. Anterior lamina cribrosa insertion in primary open-angle glaucoma patients and healthy subjects. PLoS One 2014;9:e114935.
[34] Yang H, Downs JC, Girkin C, et al. 3-D histomorphometry of the normal and early glaucomatous monkey optic nerve head: lamina cribrosa and peripapillary scleral position and thickness. Invest Ophthalmol Vis Sci 2007;48:4597–607.
[35] Burgoyne CF, Downs JC, Bellezza AJ, et al. The optic nerve head as a biomechanical structure: a new paradigm for understanding the role of IOP-related stress and strain in the pathophysiology of glaucomatous optic nerve head damage. Prog Retin Eye Res 2005; 24:39–73.
[36] Kim DM, Seo JH, Kim SH, Hwang SS. Comparison of localized retinal nerve fiber layer defects between a low-teen intraocular pressure group and a high-teen intraocular pressure group in normal-tension glaucoma patients. J Glaucoma 2007;16:293–6.
[37] Yamazaki Y, Koide C, Miyazawa T, et al. Comparison of retinal nerve-fiber layer in high- and normal-tension glaucoma. Graefes Arch Clin Exp Ophthalmol 1991;229:517–20.
[38] Kubota T, Khalil AK, Honda M, et al. Comparative study of retinal nerve fiber layer damage in Japanese patients with normal- and high-tension glaucoma. J Glaucoma 1999;8:363–6.
[39] Gramer E, Althaus G, Leydhecker W. [Site and depth of glaucomatous visual field defects in relation to the size of the neuroretinal edge zone of the optic disk in glaucoma without hypertension, simple glaucoma, pigmentary glaucoma. A clinical study with the Octopus perimeter 201 and the optic nerve head analyzer]. Klin Monbl Augenheilkd 1986;189:190–8.
[40] Caprioli J, Spaeth GL. Comparison of visual field defects in the low-tension glaucomas with those in the high-tension glaucomas. Am J Ophthalmol 1984;97:730–7.
[41] Caprioli J, Spaeth GL. Comparison of the optic nerve head in high- and low-tension glaucoma. Arch Ophthalmol 1985;103:1145–9.
[42] Hitchings RA, Anderton SA. A comparative study of visual field defects seen in patients with low-tension glaucoma and chronic simple glaucoma. Br J Ophthalmol 1983;67:818–21.
[43] Cho HK, Kee C. Comparison of the progression rates of the superior, inferior, and both hemifield defects in normal-tension glaucoma patients. Am J Ophthalmol 2012;154:958–68.e1.